Heliyon 8 (2022) e11386

Contents lists available at ScienceDirect

Heliyon

journal homepage: www.cell.com/heliyon

Research article

Enhanced optical properties of yttrium aluminum garnet with the yttrium vanadate impurity phase

Monika Skruodiene [a,*], Ruta Juodvalkyte [b], Meldra Kemere [a], Rimantas Ramanauskas [c], Anatolijs Sarakovskis [a], Ramunas Skaudzius [b]

[a] Institute of Solid State Physics, University of Latvia, LV1063 Riga, Latvia
[b] Institute of Chemistry, Vilnius University, LT-03225 Vilnius, Lithuania
[c] State Research Institute Center for Physical Sciences and Technology, LT-10257 Vilnius, Lithuania

HIGHLIGHTS

- YAG:Eu with YVO_4:Eu can be synthesized in "one pot" by a sol-gel route.
- YVO_4:Eu impurity phase can improve YAG:Eu optical properties when excited at 395 nm.
- YVO4:Eu can change luminescent decay kinetics of the composite in 395 nm wavelength.

ARTICLE INFO

Keywords:
Sol-gel synthesis
YAG:Eu
YVO_4:Eu
Modifying
Optical properties

ABSTRACT

Yttrium aluminum garnet doped with europium with an additional impurity phase of yttrium vanadate doped europium has been prepared in different ways: synthesized by a sol-gel route and mechanically mixed in a mortar. The obtained samples were characterized by X-ray diffraction analysis, and scanning electron microscopy. Photoluminescence spectra were recorded to understand the role of the impurity phase in the garnet's optical properties. The impurity phase showed a significant contribution to the optical properties of $Y_3Al_5O_{12}$:1%Eu.

1. Introduction

Garnet, due to its crystalline structure, is a very popular and important matrix for optical applications. A huge variation of transition and/or rare-earth ions could be successfully doped into this matrix. Garnets were discussed and attracted very much attention over years, however, this interest continues even today. Yttrium aluminum garnet is an interesting laser host material because of its chemical and thermal stability. As a result of the need for new versatile phosphors, there are a lot of studies made on how to modify and improve the optical properties of the phosphors. The diversity of doping exploration is very important to the development of material science. Doping YAG with V^{5+} ions often can result in the appearance of an impurity phase, since the synthesis of the YAG, with better optical properties, mostly needs a higher sintering temperature than a synthesis of tetragonal yttrium vanadium oxide YVO_4. YVO_4 is another largely explored matrix for phosphors which has attracted a great deal of interest because of its valuable characteristics such as higher chemical stability and good thermal and optical properties. YVO_4 doped with rare earths are used for micro-lasers and diode laser-pumped solid-state lasers [1, 2, 3, 4, 5, 6, 7, 8, 9].

The composite or mixture of different phases is one of the options to extend the optical and other properties [10]. The impurity phase could be added during the synthesis or mechanically mixed in a mortar. Therefore, in the present work, the concentration influence of YVO_4, as an impurity phase, on the luminescence properties of Eu^{3+} doped YAG and YVO_4 composite, synthesized *via* sol-gel assisted by molten-salt route or obtained by mechanically mixing two different compounds, is discussed in detail.

2. Experimental

2.1. Synthesis procedure

Investigated materials were synthesized by sol-gel assisted by the molten-salt route. Starting materials: $Y(NO_3)_3{\cdot}6H_2O$ (Aldrich, 99.99%),

* Corresponding author.
E-mail address: monika.skruodiene@ftmc.lt (M. Skruodiene).

https://doi.org/10.1016/j.heliyon.2022.e11386
Received 7 July 2022; Received in revised form 28 September 2022; Accepted 28 October 2022

V_2O_5 (Aldrich, 99.99%), $Al(NO_3)_3{\cdot}9H_2O$ (Roth, $\geq$ 98%), Eu_2O_3 (Aldrich, 99.99%). Flux – KCl (ACS reagent, 99.0%), complexing agent – $C_6H_8O_7{\cdot}H_2O$ (Penta, 99.5%). All nitrates were dissolved in the water at 70–80 °C temperature. V_2O_5 and Eu_2O_3 were dissolved in hot diluted HNO_3. Later HNO_3 was evaporated, and distilled water was added, to remove the excess nitric acid. The solution was stirred with a magnetic stirrer for approximately 2 h. After, $C_6H_8O_7{\cdot}H_2O$ (at a molar ratio of 1:1 to all metal ions) was added. The formed sol was stirred for 1 h at 70–80 °C, after the sol was stirred at room temperature for 24 h the solution was evaporated close to dryness. Finally, the sol was dried in a drying furnace at 140 °C temperature for 24 h. Xerogel, which became dry and porous, was ground in a mortar and annealed. The sample was calcinated at 600 °C for 2 h in air, with 5 °C/min heating rate. Later it was pre-ground and mixed with potassium chloride (10:1 ratio to reagents) and sintered 1300 °C for 4 h in air, with 5 °C/min heating rate.

The detailed steps of the synthesis route and annealing temperature followed the previously reported synthesis procedure [11]. The simplified scheme of the sol-gel technique is presented in the illustration below.

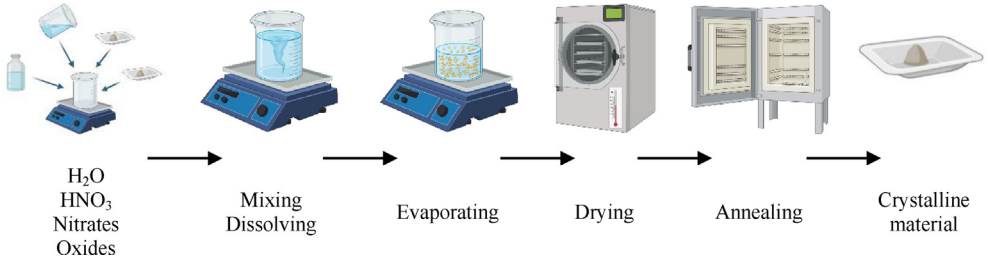

Synthesized samples were weighed according to the formula:

$Y_3Al_5O_{12}$:1%Eu (YAG:Eu); YVO_4:1%Eu (YVO:Eu); $Y_3Al_{4.5}V_{0.5}O_{12}$:1% Eu (YAG:Eu_0.5V_S); $Y_3Al_4V_1O_{12}$:1%Eu (YAG:Eu_1.0V_S); $Y_3Al_3V_2$-O_{12}:1%Eu (YAG:Eu_2.0V_S).

Mechanically mixed samples were mixed according to the data obtained from Rietveld analysis: $Y_3Al_5O_{12}$:1%Eu:YVO:1%Eu(19:1) (YAG:Eu_0.5V_M); $Y_3Al_5O_{12}$:1%Eu:YVO:1%Eu(9:1) (YAG:Eu_1.0V_M); $Y_3Al_5O_{12}$:1%Eu:YVO:1%Eu(13:7) (YAG:Eu_2.0V_M).

2.2. Characterization

X-ray diffraction (XRD) data were collected using Rigaku MiniFlexII diffractometer. Scanning electron microscopy (SEM) micrographs were taken using Hitachi SU-70 SEM. Detailed information is present in the previously reported characterization section [11].

Luminescence spectra were recorded on the Edinburgh Instruments FLS980 spectrometer [11]. Step size was 0.5 nm and the integration time was 0.2 s. Excitation wavelengths of 330 and 395 nm were selected while emission was monitored at 589 and 618 nm.

Luminescence decay kinetics were recorded at room temperature using tunable pulsed nanosecond Nd:YAG laser NT 342/3UV from Ekspla, and a spectrometer SR-303i-B and time-resolved CCD camera DH734-18F-A3 from Andor Technologies.

3. Results and discussion

3.1. X-ray diffraction (XRD) and rietveld analysis

The synthesized samples were characterized by the XRD method to evaluate their phase identification and purity. The main peaks were assigned to the garnet phase (COD ID # 1529037), meaning that all samples maintain a major phase with cubic crystal structure, which corresponds to Ia3d (#230) space group. Figure 1A demonstrates diffraction patterns of samples synthesized by the molten-salt assisted sol-gel route and annealed at 1300 °C in air. However, Figure 1B represents the diffraction patterns of samples that were mechanically mixed according to the data obtained from Rietveld analysis. In both parts of Figure 1A and B appearance of the additional peaks of the impurity, phase is visible. The main peaks are at $2\theta = 25.0°$, 49.8° and 62.7° and indicates the formation of the impurity phase of YVO_4 (COD ID # 9011137).

Rietveld refinement was performed in order to get more detailed information about the structure of the synthesized samples. Results confirmed the formation of the secondary phase of the tetragonal YVO_4 phase with I41/amd:2 space group in all vanadium doped samples. The impurity phase in the synthesized samples with the initial 0.5, 1.0, and 2.0 counts of vanadium were calculated to be 5 %, 10 %, and 35 % of the total mass, respectively. With the increase of YVO concentration in the samples, the primitive cell volume *V* of each component is almost constant, indicating no deviation from initial structures.

3.2. Scanning electron microscopy analysis

SEM analysis was obtained to analyze and compare the morphology and the particle size of synthesized and mechanically mixed powders. Figure 2A represents YAG:Eu. It possesses well-shaped irregular sphere-like morphology. The pores, clearly visible in Figure 2A and C, could be formed by the escaping gasses during the decomposition of the organic components and residual nitrates. It can be observed that most of the particles are in a size range between 200 and 800 nm. Meanwhile, YVO:Eu possesses irregular, slightly angular, sphere-like morphology with clear boundaries between each particle (Figure 2B). The particle size is much bigger, about 1.7–6 μm. Figure 2C and D correspond to YAG:Eu_1.0V_S and YAG:Eu_1.0V_M samples, respectively. Two groups of particles of different sizes and shapes are clearly visible from the figures. Note that during synthesis obtained composite 0.5–4 μm size particles of YVO are located on the surface and it seems they have stuck and even sunk in the particles of garnet (Figure 2C), meanwhile the particles of each component of the composite are separate in Figure 2D.

3.3. Luminescence properties

The emission spectra were recorded under λ_{ex} = 330 and 395 nm excitation. In the emission spectra (Figure 3) peaks at 589 nm, 593 nm ($^5D_0 \rightarrow {}^7F_1$), 608 nm, 614 nm, 618 nm ($^5D_0 \rightarrow {}^7F_2$), 697 nm, 703 nm, and 709 nm ($^5D_0 \rightarrow {}^7F_4$) are clearly visible. The first obvious indication is that YVO exhibits higher emission compared to YAG irrespective to the excitation wavelength. Also, there are some changes in the emission spectra of the samples if the emission is monitored for Eu^{3+} under 395 nm excitation in YAG, as compared to the emission Eu^{3+} in YVO. Two bands with maxima ca. 589 and 709 nm are visible. They are typical bands for Eu^{3+} in the YAG matrix and remain in the emission spectra of any composite under 395 nm excitation. The result of integrated intensity evidently concludes that YVO is the better matrix for europium than YAG. Nevertheless, the addition of vanadium to the YAG structure has staggering impact on the emission resulting in dominant peaks at the

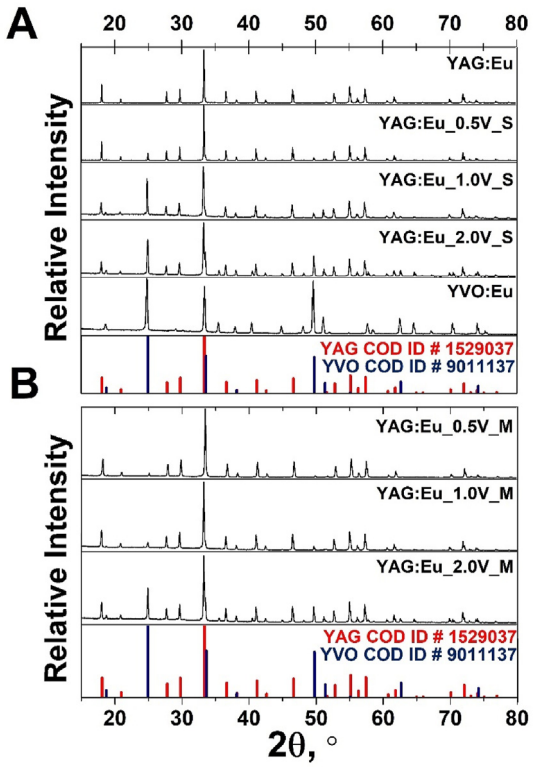

Figure 1. XRD patterns of YAG:Eu, YVO:Eu, and A – samples synthesized by sol-gel route, B – mechanically mixed samples.

positions characteristic of YVO under 330 nm or 395 nm excitation and remaining YAG peaks under 395 nm excitation. Note, that although the size of YVO particle is larger in the composites obtained by mechanical method, the integrated emission of the composites synthesized *via* sol-gel assisted by molten-salt route are slightly higher.

Luminescence properties were investigated by measuring the photoluminescence decay curves of the samples. Most of them (Figure 4A.) exhibit bi-exponential photoluminescence decay. It indicates that there should be two different depopulation mechanisms of Eu^{3+} excited states. YAG:Eu bi-exponential lifetime parameter ratio (τ_1/τ_2, %) is 30/70, where τ_2 is dominant, meanwhile YVO:Eu is mono-exponential. However, τ_1 becomes dominant in the composites. The PL decay curves become steeper with increasing YVO impurity phase concentration indicating that the lifetime of the excited state becomes shorter. The shortened decay times usually correspond to decreased efficiency of the activator ions.

Besides, all synthesized samples containing YVO possess a significant rise in decay time (inset Figure 4A). The increment of the emission intensity is related to the increment of the number of the excited activator ions over time. It proves additional excited state lifetime measurement, where samples were illuminated with a short pulse of light and the intensity of the emission versus time was recorded (Figure 4B). In our case, the PL decay curves were measured for the $^5D_0 \rightarrow {}^7F_2$ transitions. It is most likely that this additional population of $^5D_0$ states is caused by non-radiative relaxation from higher energy levels. Moreover, it may also indicate the interaction between the YAG and YVO matrixes, since the peak positions observed in emission spectra are characteristic for YVO phase even within small amounts of vanadium in composite. Decay rise time does not appear in mechanically mixed samples with a high concentration of impurity phase probably due to less homogeneity of the composites and smaller surface of interaction between different components.

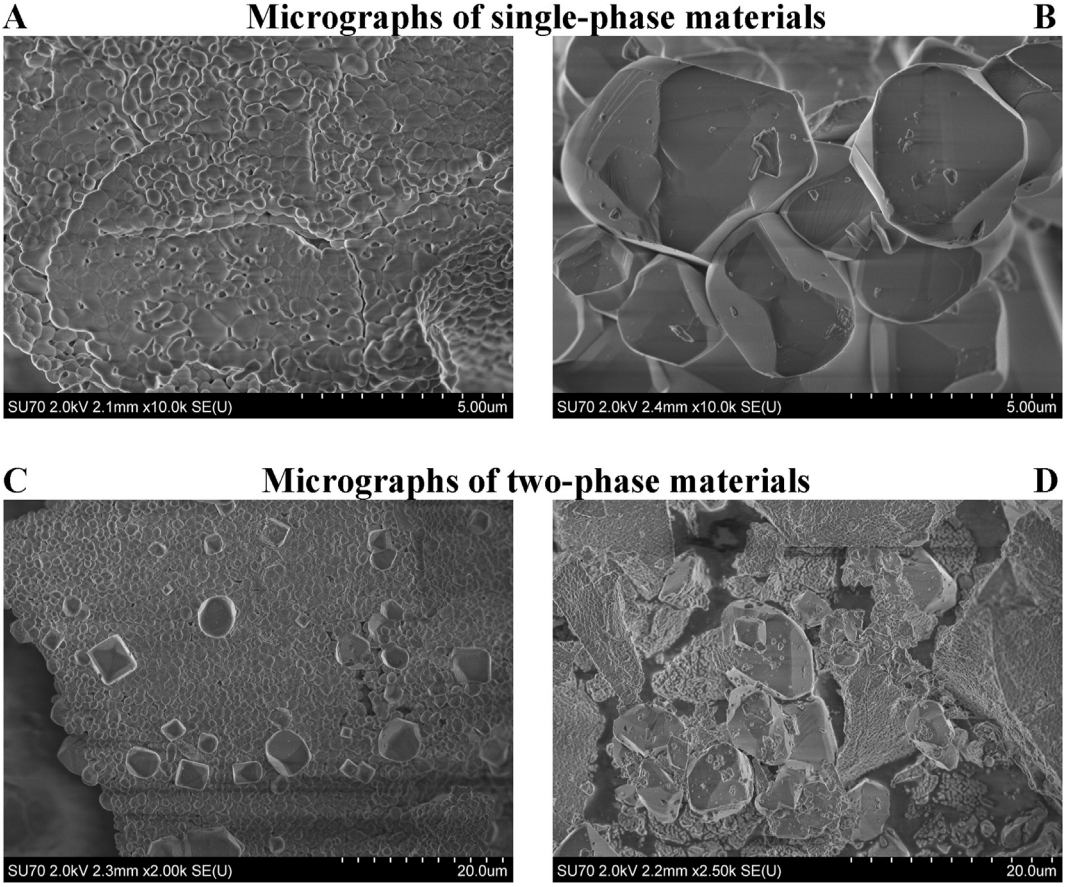

Figure 2. SEM images of powder the samples, YAG:Eu (A), YVO:Eu (B), YAG:Eu_1.0V_S (C) and YAG:Eu_1.0V_M (D).

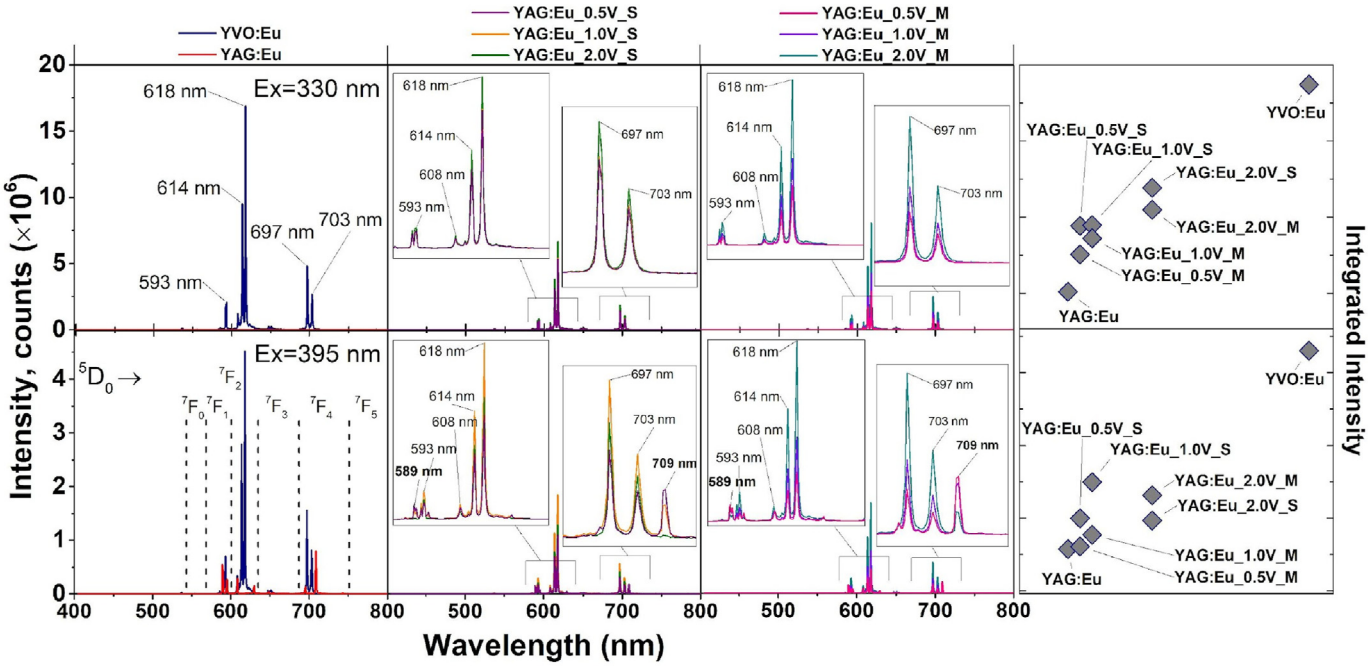

Figure 3. Emission spectra of the samples. Integrated emission intensity is on the right.

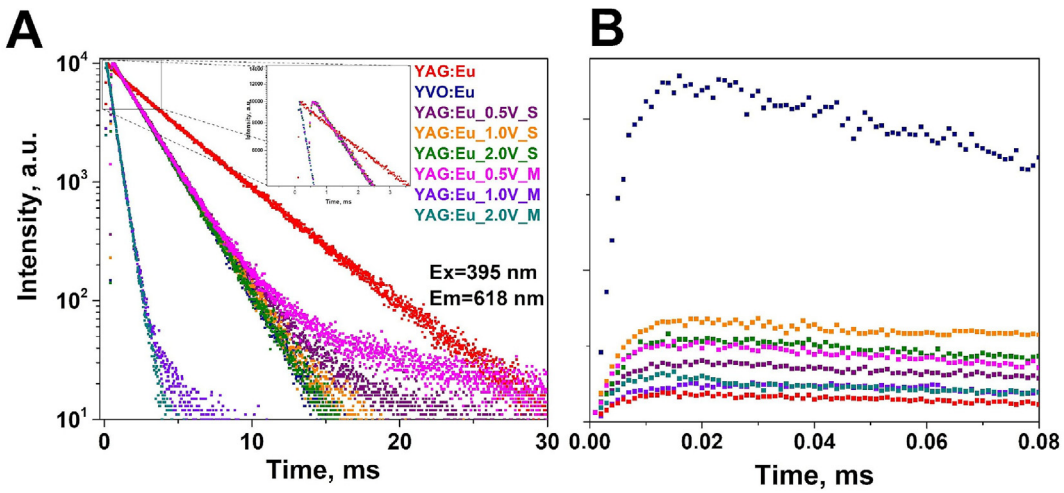

Figure 4. Luminescent decay curves (A) and luminescence lifetime of Eu^{3+} (B) of the samples.

4. Conclusions

In this study yttrium aluminum garnet was modified by adding vanadium into the structure. XRD analysis and Rietveld refinement clearly indicated that instead of the successful incorporation of vanadium into the garnet structure, the secondary phase of YVO was observed. The impurity phase was also clearly observed in the SEM images. The investigation of the morphology of the synthesized and mechanically mixed composites revealed that the composites obtained by chemical route are more homogeneous. The investigation of the luminescence properties demonstrated that the appearance of YVO in the composite gives a staggering impact on the emission resulting in higher intensity even under 330 nm excitation. The peak positions of the emission for the composite with dominant garnet phase are characteristic to YVO phosphors. Moreover, the change in decay time indicates the interaction between YAG and YVO phases, resulting in the decay rise time. The additional investigation to confirm this is required as well as the vanadium amount could be reduced to ppm in the composite. The synthesis by a simple aqueous sol-gel route assisted by molten-salt method should be chosen, since the results of the composites according to integrated emission were slightly better.

Declarations

Author contribution statement

Monika Skruodiene: Conceived and designed the experiments; Performed the experiments; Analyzed and interpreted the data; Wrote the paper.

Ruta Juodvalkyte: Performed the experiments.

Meldra Kemere: Analyzed and interpreted the data.

Rimantas Ramanauskas: Contributed reagents, materials, analysis tools or data; Wrote the paper.

Anatolijs Sarakovskis, Ramunas Skaudzius: Analyzed and interpreted the data; Contributed reagents, materials, analysis tools or data; Wrote the paper.

Funding statement

Dr Monika Skruodiene was supported by ERDF [1.1.1.2/VIAA/3/19/480]. This work was supported by Horizon 2020 Framework Programme [H2020-WIDESPREAD-01-2016-2017-TeamingPhase2].

Data availability statement

Data included in article/supplementary material/referenced in article.

Declaration of interests statement

The authors declare no conflict of interest.

Additional information

No additional information is available for this paper.

References

[1] M. Maçzka, A. Bednarkiewicz, E. Mendoza-Mendoza, A.F. Fuentes, L. Kępiński, Low-temperature synthesis, phonon and luminescence properties of Eu doped $Y_3Al_5O_{12}$(YAG) nanopowders, Mater. Chem. Phys. 143 (2014) 1039–1047.

[2] B.F. dos Santos, R.M. Araujo, M.E.G. Valerio, M.V.D.S. Rezende, Optical spectroscopy study of YVO_4:Eu^{3+} nanopowders prepared by the proteic sol-gel route, Solid State Sci. 42 (2015) 45–51.

[3] R.F. Likerov, V.F. Tarasov, A.A. Sukhanov, R.M. Eremina, K.B. Konov, I.v. Yatsyk, A.v. Shestakov, Y.D. Zavartsev, S.A. Kutovoi, Investigation of neodymium doped YVO_4 by EPR method, Opt. Mater.(Amst) 85 (2018) 414–417.

[4] Z. Xu, X. Kang, C. Li, Z. Hou, C. Zhang, D. Yang, G. Li, J. Lin, Ln^{3+} (Ln = Eu, Dy, Sm, and Er) ion-doped YVO_4 nano/microcrystals with multiform morphologies: hydrothermal synthesis, growing mechanism, and luminescent properties, Inorg. Chem. 49 (2010) 6706–6715.

[5] J. Ma, M. Du, F. Miao, Spectroscopic investigation of YAG crystal doped with tetrahedrally coordinated V^{3+} ions, Phys. Status Solidi (b) 243 (8) (2006) 1785–1790.

[6] Y. Hua, W. Zhuang, H. Ye, D. Wang, S. Zhang, X. Huang, A novel red phosphor for white light emitting diodes, J. Alloys Compd. 390 (2005) 226–229.

[7] M. He, J. Jia, J. Zhao, X. Qiao, J. Du, X. Fan, Glass-ceramic phosphors for solid state lighting: a review, Ceram. Int. 47 (2021) 2963–2980.

[8] A. Pakalniskis, A. Marsalka, R. Raudonis, V. Balevicius, A. Zarkov, R. Skaudzius, A. Kareiva, Sol-gel synthesis, and study of praseodymium substitution effects in yttrium aluminum garnet $Y_{3-x}Pr_xAl_5O_{12}$, Opt. Mater. 111 (2021), 110586.

[9] K. Kniec, L. Marciniak, The influence of grain size and vanadium concentration on the spectroscopic properties of YAG:V^{3+},V^{5+} and YAG: V, Ln^{3+} (Ln^{3+} = Eu^{3+},Dy^{3+}, Nd^{3+}) nanocrystalline luminescent thermometers, SeAc B 264 (2018) 382–390.

[10] P. Jiang, J. Ni, H. Zhang, H. Qi, W. Wang, Z. Song, J. Guo, G. Peng, C. Wang, High-power and high-energy Nd:YAG-Nd:YVO_4 hybrid gain Raman yellow laser, Opt Express 28 (2020), 24088.

[11] M. Skruodiene, R. Juodvalkyte, G. Inkrataite, A. Pakalniskis, R. Ramanauskas, A. Sarakovskis, R. Skaudzius, Sol-gel assisted molten-salt synthesis of novel single phase $Y_{3-2x}Ca_{2x}Ta_xAl_{5-x}O_{12}$:1%Eu garnet structure phosphors, J. Alloys Compd. 890 (2022).

The Institute of Solid State Physics, University of Latvia (Latvia), as the Centre of Excellence has received funding from the European Union's Horizon 2020 Frame-work Programme H2020-WIDESPREAD-01-2016-2017-Teaming Phase2 under grant agreement No. 739508, project CAMART2